MICROVASCULAR RESEARCH 44, 143–165 (1992)

Interstitial Pressure, Volume, and Flow during Infusion into Brain Tissue

PETER J. BASSER

Mechanical Engineering Section, Biomedical Engineering and Instrumentation Program, National Institutes of Health, Bethesda, Maryland 20892

Received January 13, 1992

A model of infusion-induced swelling in the brain is presented, in which gray and white matter are treated as poroelastic media. The distributions of interstitial pressure, flow, and volume are derived for steady-state and transient infusion protocols. A significant percentage increase in interstitial volume is predicted near the injection site, despite only a modest increase in tissue-averaged fluid content there. The model also can be used to estimate mechanical parameters of brain tissue, such as its hydraulic permeability, shear modulus, and Lamé constant. A solute transport equation that incorporates tissue swelling is also presented. This work suggests that knowing the distribution of swelling induced by infusion is a prerequisite to describing interstitial transport of solutes.

INTRODUCTION

It was proposed recently that infusing chemotherapeutic agents into the interstitium of the brain may enhance their efficacy [1]. This suggestion raises interesting questions: Can interstitial solute concentration be predicted in gray or white matter during infusion? How does the therapeutic benefit depend on infusion pressure, flow rate, or the material properties of brain tissue? Before addressing these questions we must understand a more fundamental process. Infusion induces tissue swelling. Swelling alters interstitial solute transport.

For the purpose of describing infusions, models of solute transport within extracellular spaces do not describe tissue mechanics adequately. For example, the interstitial transport models of Taylor [2,3] and Nicholson [4] do not explicitly satisfy Newton's second and third laws of motion. Conversely, models of brain mechanics that do satisfy $\boldsymbol{F} = m\,\boldsymbol{a}$ and that contain mechanical boundary conditions typically do not incorporate solute transport equations [5–8]. Here, we synthesize the viewpoints of chemical and mechanical engineers, coupling tissue swelling with solute transport.

To describe infusion-induced swelling, we use an established model of consolidation, Biot's equations [9,10], to derive analytical expressions for the distribution of tissue displacement, interstitial pressure, flow, and volume in gray and white matter following steady-state and transient infusion from a spherical cavity. We then describe transport of an infused solute in this swelling tissue. No free

0026-2862/92 $5.00

parameters are used; material parameters are taken from published data whenever possible.

In Section 1, the Biot model of consolidation is derived from basic principles; in Section 2, it is adapted to describe infusion into an infinite isotropic medium. Sections 3–7 contain analytical solutions for interstitial pressure, fluid velocity, and extracellular fraction during steady-state and transient infusion into brain tissue. Section 8 describes how tissue swelling induced by infusion can be incorporated into a solute transport equation.

NOMENCLATURE

r	=	Radial distance	(cm)
a	=	Radius of spherical cavity	(cm)
R_0	=	Radius of tissue sample	(cm)
t	=	Time	(sec)
$\mathbf{u}$	=	Tissue displacement vector	(cm)
$\mathbf{V}$	=	Interstitial velocity vector	(cm/sec)
$\boldsymbol{\tau}$	=	Effective stress tensor	(dynes/cm^2)
$\boldsymbol{\varepsilon}$	=	Network strain tensor	(dimensionless)
e	=	Network dilatation	(dimensionless)
P	=	Interstitial pore fluid pressure	(dynes/cm^2)
$\mathbf{I}$	=	Identity tensor	(dimensionless)
P_0	=	Infusion pressure	(dynes/cm^2)
Q_0	=	Volume flow rate	(cm^3/sec)
f	=	Interstitial fluid volume fraction	(dimensionless)
G	=	Elastic shear modulus (at $P = 0$)	(dynes/cm^2)
λ	=	Lamé constant (at $P = 0$)	(dynes/cm^2)
ν	=	Poisson ratio (at $P = 0$)	(dimensionless)
κ	=	Hydraulic conductivity (permeability)	(cm^4/dynes-sec)
c	=	Network consolidation constant	(cm^2/sec)
τ_c	=	Consolidation time constant	(sec)
τ_a	=	Advective time constant	(sec)
τ_d	=	Diffusive time constant	(sec)
C'	=	*Interstitial* solute concentration	(mole/cm^3)
C_t	=	Spefic tissue compliance	(cm^2/dynes)
D	=	Diffusivity	(cm^2/sec)
R	=	Hydraulic input resistance	(dynes-sec/cm^5)
V_{0T}	=	Undeformed tissue volume	(cm^3)
V_T	=	Deformed tissue volume	(cm^3)
V_{f0}	=	Undeformed pore volume	(cm^3)
V_f	=	Deformed pore volume	(cm^3)
ϕ_s	=	Rate of production of solute	(moles/cm^3/sec)
ϕ_r	=	Rate of removal of solute	(moles/cm^3/sec)

N. B.: $P = 0$ corresponds to ambient CSF pressure

THEORY

1. Biot's Consolidation Model

Since M. A. Biot proposed a three-dimensional continuum model of soil consolidation [9–14], consolidation models have been used widely to predict the mechanics of artery wall [15–17], bone [18], brain [5–8], cartilage [19], synthetic hydrogels [20,21], and rocks [22]. Biot's model of consolidation [9] is used here to describe the dynamic response of brain tissue to fluid infusion.

Brain tissue is modeled as a fluid-saturated, homogeneous poroelastic medium—an elastic network with communicating, fluid-filled pores [5–8]. The model contains a linear constitutive law of the elastic network, Darcy's law of fluid flow in a porous medium, and the equations of conservation of mass and momentum as applied to the network and the interstitial fluid.

The tissue, which is composed of interstitial fluid, elastic fibers, and cells is assumed to be compressible and isotropic. It obeys a linear constitutive law [12],

$$\tau = 2G\varepsilon + \lambda e\mathbf{I} - P\mathbf{I}. \tag{1.1}$$

In Eq. (1.1), τ is the Terzaghi or effective stress tensor [23,24] of tissue, G and λ are the Lamé constants of the elastic network, P is the pore fluid pressure, and $\mathbf{I}$ is the identity tensor. The network dilatation, e, is the divergence of the network displacement vector, $\mathbf{u}$:

$$e = \mathrm{Tr}(\varepsilon) = \nabla \cdot \mathbf{u}. \tag{1.2}$$

The infinitesimal network strain tensor, ε, is the symmetric part of the gradient of the displacement vector:

$$\varepsilon = \frac{1}{2}(\nabla \mathbf{u} + (\nabla \mathbf{u})^{\mathrm{T}}). \tag{1.3}$$

Above, the superscript "T" in Eq. (1.3) and "Tr" in Eq. (1.2) signify the transpose and trace operations, respectively.

It is assumed that the infusate has the same ionic composition and osmolarity as CSF. Nevertheless, osmotic pressure can be incorporated naturally into Eq. (1.1) by including it as an additional isotropic pressure [25], and so can the isotropic chemical stress caused by variations in local ionic strength or pH [25].

Since inertia is negligible [20], the three equations of mechanical equilibrium are given by

$$\nabla \cdot \tau = \mathbf{0}. \tag{1.4}$$

Substituting the constitutive law, Eq. (1.1), and the definition of strain, Eq. (1.3), into the equilibrium equation, Eq. (1.4), we obtain Navier's equations for the network displacement proposed by Biot [12]:

$$G\nabla^2\mathbf{u} + (G + \lambda)\nabla(\nabla \cdot \mathbf{u}) - \nabla P = \mathbf{0}. \tag{1.5}$$

Taking the divergence of Eq. (1.5), we obtain

$$G\nabla \cdot \nabla^2\mathbf{u} + (G + \lambda)\nabla \cdot \nabla(\nabla \cdot \mathbf{u}) - \nabla \cdot \nabla P = 0. \tag{1.6}$$

Recalling that $\nabla \cdot \nabla = \nabla^2$ and using Eq. (1.2),

$$\nabla \cdot \nabla^2 \mathbf{u} = \nabla \cdot \nabla (\nabla \cdot \mathbf{u}) = \nabla^2 e, \tag{1.7}$$

we relate the tissue pressure and dilatation [12]:

$$(2G + \lambda) \nabla^2 e = \nabla^2 P. \tag{1.8}$$

Biot calls the coefficient of $\nabla^2 e$ in Eq. (1.8) "¼" [12], but expresses it in terms of G and ν, the Poisson ratio.[1]

It is assumed that both the constituents of the network and the fluid are individually incompressible in brain tissue [5–8] so the equation of conservation of mass for the *tissue* therefore becomes

$$\nabla \cdot \left((1 - f) \frac{\partial \mathbf{u}}{\partial t} + f \mathbf{V} \right) = 0 = \nabla \cdot \left(\frac{\partial \mathbf{u}}{\partial t} + f \left(\mathbf{V} - \frac{\partial \mathbf{u}}{\partial t} \right) \right), \tag{1.9}$$

where f is the volume fraction of fluid (pores) in the undeformed tissue, and $\mathbf{V}$ is the velocity of the interstitial fluid measured in the laboratory frame. In the linear theory, f is constant, so that

$$(1 - f) \frac{\partial e}{\partial t} + f \nabla \cdot \mathbf{V} = 0. \tag{1.10}$$

The relative velocities of the interstitial fluid and network are related to the pore pressure gradient using Darcy's law [13],

$$f \left(\mathbf{V} - \frac{\partial \mathbf{u}}{\partial t} \right) = - \kappa \nabla P, \tag{1.11}$$

where the permeability, κ, is assumed constant. Equation (1.11) implies that a gradient in pore pressure accompanies a relative velocity between the interstitial fluid and the network. One can include osmotic pressure in Darcy's law if necessary [25]. Taking the divergence of Eq. (1.11),

$$f \left(\nabla \cdot \mathbf{V} - \frac{\partial e}{\partial t} \right) = - \kappa \nabla^2 P, \tag{1.12}$$

and using Eqs. (1.8), (1.10), and (1.12), we derive the consolidation equation of Biot [12],

$$\frac{\partial e}{\partial t} = \kappa (2G + \lambda) \nabla^2 e. \tag{1.13}$$

Biot called the factor $\kappa (2G + \lambda)$ the coefficient of consolidation,[2] c. It is the diffusivity of dilatation, and is both analogous to and has the same units as a chemical or thermal diffusivity.

In this study, Darcy's law and the equations of conservation of mass and momentum, Eqs. (1.11), (1.10), and (1.5), are solved simultaneously for the tissue displacement, fluid velocity, and pore pressure, using boundary and initial con-

[1] Biot actually used "$1/a = 2G(1 - \nu)/(1 - 2\nu)$" [12], where ν is the Poisson ratio of the consolidated poroelastic material; but it is easy to show that "$1/a$" $= (2G + \lambda)$ by using the definition $\nu = \lambda/2(G + \lambda)$, where λ is the Lamé constant.

[2] Biot used the definition $c = \kappa/a$; however, it is easy to show that $c = \kappa(2G + \lambda)$ by using $\nu = \lambda/2(G + \lambda)$.

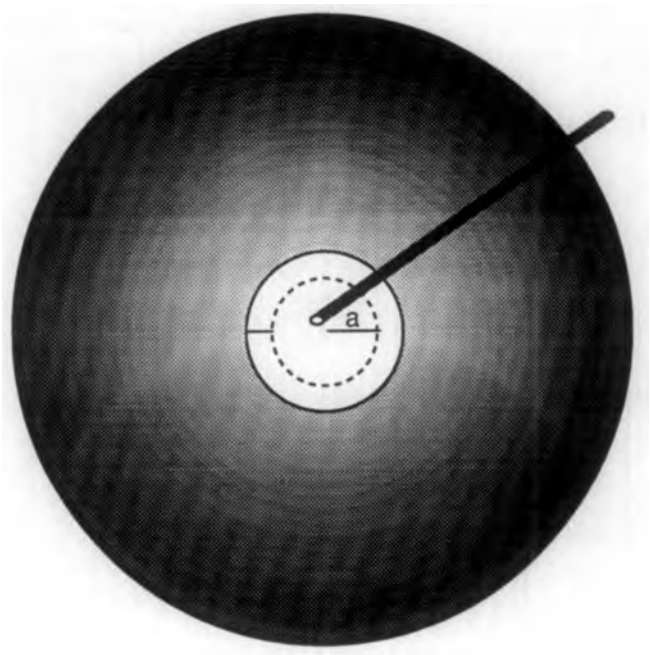

FIG. 1. The spherical pore of radius a within an infinite poroelastic tissue sample. During infusion, the tissue swells and cavity radius increases by $u_r(a)$.

ditions appropriate for a particular fluid-infusion protocol. Once the displacement is known, the tissue swelling and interstitial volumes are calculated.

Capillary filtration is ignored in this model because estimates of permeability [26] suggest that loss through filtration is several orders of magnitude smaller than the volume flow rate of the infusate [1]. The blood–brain barrier also prevents the infused chemotherapeutic agents from being absorbed and cleared through the vasculature [1]. Since brain tissue contains no lymphatics, we can ignore this clearance mechanism as well.

Although it has been assumed that both the network and the interstitial fluid are individually incompressible [5–8], the vasculature is a third compressible phase that may add compliance to brain tissue. In principle, the vasculature can be incorporated into this model by treating it as a though it were a compressible gas [9]. To mitigate the effect of vascular compliance, we can use material properties measured at mean capillary pressure.

2. Consolidation in an Infinite, Isotropic Medium

For injection into a homogeneous, isotropic poroelastic medium, the equations take on a simple form. As is shown in Fig. 1, fluid is assumed to be infused in either gray or white matter through a spherical cavity of radius a in the unstressed state. We assume that the applied stress at the tissue/cavity boundary is radially symmetric and that the displacement, fluid velocity, and strain fields are as well. Therefore, shear strains all vanish, i.e., $\varepsilon_{r\phi} = \varepsilon_{\phi r} = \varepsilon_{\phi\theta} = \varepsilon_{\theta\phi} = \varepsilon_{r\theta} = \varepsilon_{\theta r} = 0$. Only the diagonal elements of the network strain tensor, $\boldsymbol{\varepsilon}$, survive:

$$\varepsilon_{rr} = \frac{\partial u_r}{\partial r}, \qquad \varepsilon_{\phi\phi} = \frac{u_r}{r}, \qquad \varepsilon_{\theta\theta} = \frac{u_r}{r}, \tag{2.1}$$

where u_r is the network displacement in the radial direction, and ε_{rr}, $\varepsilon_{\phi\phi}$, and $\varepsilon_{\theta\theta}$ are the normal strains in the radial, longitudinal, and latitudinal coordinate directions, respectively. The dilatation, e, is given by their sum (as in Eq. (2.1)),

$$e = \frac{\partial u_r}{\partial r} + \frac{2u_r}{r} = \frac{1}{r^2}\frac{\partial}{\partial r}(r^2 u_r). \tag{2.2}$$

The equation of conservation of momentum in the radial direction, Navier's equation (1.5), reduces to

$$(2G + \lambda)\frac{\partial}{\partial r}\left(\frac{1}{r^2}\frac{\partial}{\partial r}(r^2 u_r)\right) = (2G + \lambda)\frac{\partial e}{\partial r} = \frac{\partial P}{\partial r}, \tag{2.3}$$

and its divergence, Eq. (1.6), is given by

$$(2G + \lambda)\frac{1}{r^2}\frac{\partial}{\partial r}\left(r^2\frac{\partial e}{\partial r}\right) = \frac{1}{r^2}\frac{\partial}{\partial r}\left(r^2\frac{\partial P}{\partial r}\right). \tag{2.4}$$

The equation of conservation of mass, Eq. (1.10), is now

$$\frac{1}{r^2}\frac{\partial}{\partial r}\left(r^2\left((1 - f)\frac{\partial u_r}{\partial t} + fV_r\right)\right) = 0. \tag{2.5}$$

Darcy's law of fluid flow, Eq. (1.11), becomes

$$f\left(V_r - \frac{\partial u_r}{\partial t}\right) = -\kappa\frac{\partial P}{\partial r}. \tag{2.6}$$

The consolidation equation, (1.13), is given by

$$\frac{\partial e}{\partial t} = c\frac{1}{r^2}\frac{\partial}{\partial r}\left(r^2\frac{\partial e}{\partial r}\right). \tag{2.7}$$

3. Boundary and Initial Conditions

Specifying boundary conditions for poroelastic medium is a source of confusion. It arises from attempting to reconcile the microcontinuum (pore length scale) and macrocontinuum (tissue length scale) descriptions. Although at an interface, the traction must be continuous, typically we know the hydrostatic pressure or the contact stress there. Generally, we apply separate conditions on the fluid and solid phases. We use a self-consistent system proposed by Kenyon [27]. For the elastic portion, the contact stress or displacement is specified. For the interstitial fluid, the pore pressure, its gradient, or some linear combination is specified.

From the constitutive law, the contact stress on the network is given as

$$\tau_{rr} = (2G + \lambda)\frac{\partial u_r}{\partial r} + \frac{2\lambda u_r}{r} = 2G\frac{\partial u_r}{\partial r} + \frac{\lambda}{r^2}\frac{\partial(r^2 u_r)}{\partial r}. \tag{3.1}$$

With the reference CSF pressure set to zero at a boundary, the interstitial pressure also vanishes:

$$P(r) = 0. \tag{3.2}$$

At an impermeable boundary the interstitial pressure gradient would be set to zero, i.e.,

$$\frac{\partial P}{\partial r}(r) = 0. \tag{3.3}$$

At the infusion site, the tissue has been cored out, creating a sphere of radius a. Fluid can be delivered to this cavity from a constant pressure or a constant flow source. In this study, it is assumed that there is no pressure drop within the cavity or at the interface with the tissue.

In a transient infusion problem, the initial deformation is isovolumic. Moreover, at the initial instant of the imposition of the flow or pressure, there is no redistribution of fluid and solid volume in the interstitium. Therefore, the initial dilatation of the network is zero, i.e.,

$$e(r, 0^+) = 0. \tag{3.4}$$

Generally the pressure or flow at the boundary $r = a$ is a time-varying function, e.g.,

$$P(a, t) = f(t) \qquad \text{or} \qquad Q(a, t) = g(t). \tag{3.5}$$

4. Infusion from a Constant Pressure Source into Tissue

Imagine that the small spherical cavity of radius a (as shown in Fig. 1), cored from the tissue, is maintained at a constant pressure, P_0. In the steady-state, the dependent variables are all independent of time; the continuity equation, Eq. (2.5), therefore becomes

$$\frac{1}{r^2}\frac{\partial}{\partial r}(r^2 V_r) = 0 \qquad \text{or} \qquad V_r = \frac{B}{r^2}, \tag{4.1}$$

where B is an unknown constant. Integrating Darcy's law, (2.6), with this velocity profile,

$$P(r) = \frac{f}{\kappa}\frac{B}{r} + C. \tag{4.2}$$

The pore pressure vanishes infinitely far from the source, so that

$$P(r) = \frac{Bf}{\kappa}\frac{1}{r}. \tag{4.3}$$

For $P(a) = P_0$, the dimensionless pressure distribution is given by

$$\frac{P(r)}{P_0} = \frac{a}{r}. \tag{4.4}$$

This solution, which satisfies Laplace's equation [13], shows that the excess pore pressure decays rapidly within a few cavity diameters from the infusion site. Figure 2 is a plot of pressure vs radial distance. The steady-state pressure distribution is identical for gray and white matter.

To find the steady-state displacement, we return to the mechanical equilibrium equation in the radial direction, Eq. (2.3), and Eq. (4.4):

$$\frac{\partial}{\partial r}\left(\frac{1}{r^2}\frac{\partial}{\partial r}(r^2 u_r)\right) = \frac{1}{2G + \lambda}\frac{\partial P}{\partial r} = -\frac{P_0}{2G + \lambda}\frac{a}{r^2}. \tag{4.5}$$

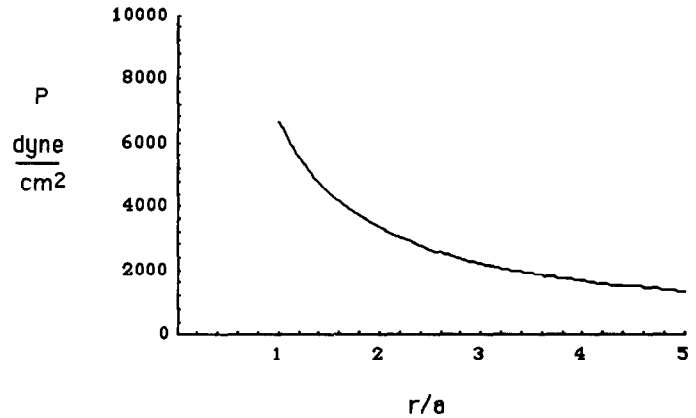

FIG. 2. The steady-state pressure, $P(r)$, vs dimensionless radius, r/a, in gray matter for a constant pressure infusion.

Its particular and homogeneous solutions add up to

$$u_r(r) = \frac{P_0 a}{2(2G + \lambda)} + \frac{D}{r^2} + C r. \tag{4.6}$$

With no contact stress on the elastic network at the cavity interface, and far from the cavity

$$(2G + \lambda)\frac{\partial u_r}{\partial r} + \frac{2\lambda u_r}{r} = 0 \qquad \text{at } r = a \text{ and } r = \infty. \tag{4.7}$$

Therefore, the steady-state displacement is

$$u_r(r) = \frac{P_0 a}{4G(2G + \lambda)r^2}(2Gr^2 + \lambda a^2) = a\frac{P_0}{2(2G + \lambda)}\left(1 + \frac{\lambda}{2G}\left(\frac{a}{r}\right)^2\right). \tag{4.8}$$

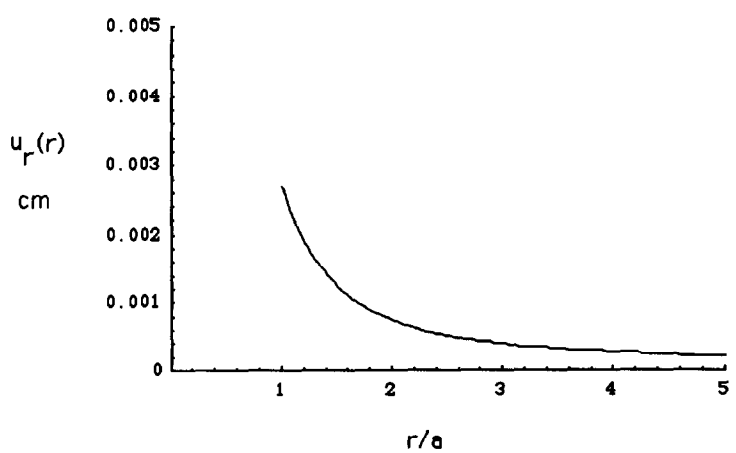

FIG. 3. The steady-state tissue displacement, $u_r(r)$, vs r/a in gray matter for a constant pressure infusion.

TABLE 1
PROPOSED MATERIAL PARAMETERS FOR GRAY AND WHITE MATTER

Infusion parameters		
$P_0 = 6664$	Infusion pressure	dynes/cm^2
$Q_0 = 10^{-5}$	Infusion flow rate	cm^3/sec
$a = 0.03$	Radius of spherical cavity	cm
$R_0 = 2$	Radius of tissue sample	cm
$D = 10^{-7}$	Solute diffusivity	cm^2/sec
Gray matter		
$G = 2 \times 10^4$	Shear modulus	dynes/cm^2
$\lambda = 9 \times 10^5$	Lamé constant	dynes/cm^2
$\kappa = 5 \times 10^{-9}$	Permeability	cm^4/dynes-sec
$f = 0.2$	Pore fraction	dimensionless
[29]		
White matter		
$G = 9 \times 10^3$	Shear modulus	dynes/cm^2
$\lambda = 4 \times 10^5$	Lamé constant	dynes/cm^2
$\kappa = 7.5 \times 10^{-9}$	Permeability	cm^4/dynes-sec
$f = 0.2$	Pore fraction	dimensionless
[29]		

Figure 3 shows the steady-state radial network displacement, $u_r(r)$, as a function of normalized radial distance, r/a, using parameters for gray matter given in Table 1. In soft gels [28] and brain tissue [5–8] it is assumed that $G \ll \lambda$. In this limit, the displacement has a $1/r^2$ dependence, as seen in Eq. (4.8). Since the radial strain, $\partial u_r/\partial r$, is negative, the tissue is in radial compression. The normal longitudinal and latitudinal strain, u_r/r, is positive, so that the tissue is in tension in these directions.

Since the network velocity is zero in the steady-state, using (4.4) and (4.1), the fluid velocity in the tissue is

$$V_r(r) = \frac{\kappa P_0 a}{r^2 f}. \tag{4.9}$$

Like displacement, fluid velocity has a $1/r^2$ dependence. Figure 4 shows the steady-state radial fluid velocity as a function of normalized radial distance, using parameters for gray matter given in Table 1.

The volume flow rate into the cavity, $Q(a)$, is deduced from the continuity equation as

$$Q(a) = f V_r(a)\, 4\pi a^2 = 4\pi a \kappa P_0. \tag{4.10}$$

We define the hydraulic resistance of the tissue, R, as the pressure in the cavity divided by the infused volume flow rate:

$$R = \frac{P_0}{Q(a)} = \frac{1}{4\pi a \kappa}. \tag{4.11}$$

This result suggests a simple experiment to determine hydraulic conductivity of the matrix, κ, by simultaneously measuring $Q(a)$ and P_0. Data plotted as

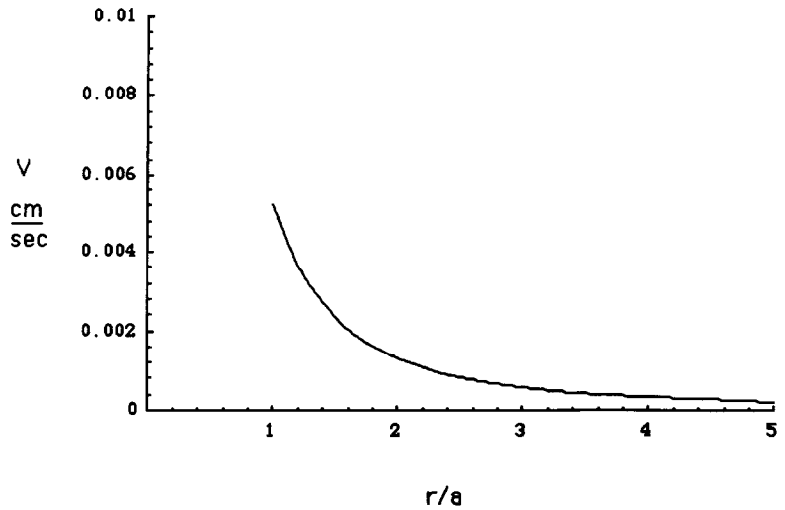

FIG. 4. The steady-state interstitial fluid velocity distribution, $V_r(r)$, vs r/a in gray matter for a constant pressure infusion.

$Q(a)/(4\pi a)$ vs P_0 should fit a line passing through the origin, the slope of which is κ.

5. Infusion from a Constant Flow Source

Imagine that the tissue is unconstrained and infused from a constant flow source, Q_0. The continuity equation becomes

$$\frac{1}{r^2}\frac{\partial}{\partial r}(r^2 V_r) = 0 \qquad \text{or} \qquad V_r(r) = \frac{B}{r^2}, \tag{5.1}$$

where B is a constant that is determined from the boundary condition

$$V_r(a) = \frac{Q_0}{4\pi a^2 f}. \tag{5.2}$$

Since the first and second equations must be simultaneously satisfied,

$$V_r(r) = \frac{Q_0}{4\pi r^2 f}. \tag{5.3}$$

Integrating Darcy's law using this velocity distribution, we obtain

$$P(r) = \frac{Q_0}{4\pi r\kappa} + C. \tag{5.4}$$

In order for the pressure to vanish at $r = \infty$,

$$P(r) = \frac{Q_0}{4\pi r\kappa}. \tag{5.5}$$

Figure 5 is a plot of $P(r)$ vs r, Eq. (5.5), using parameters for gray matter in Table 1. The pressure distribution depends upon permeability.

The steady-state infusion pressure in the cavity is

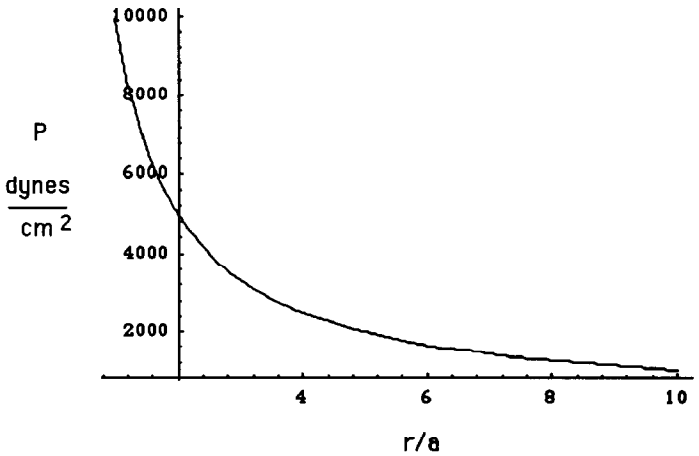

FIG. 5. The steady-state pressure, $P(r)$, vs r/a, in gray matter for a constant flow-rate infusion.

$$P(a) = \frac{Q_0}{4\pi a\kappa}, \tag{5.6}$$

and the resistance is now given by

$$R = \frac{1}{4\pi a\kappa} = \frac{P(a)}{Q_0}; \tag{5.7}$$

therefore, a constant flow infusion also can be used to estimate κ.

To find the steady-state displacement, we return to the mechanical equilibrium equation for the radial direction, Eq. (2.3), and Eq. (5.5):

$$\frac{\partial}{\partial r}\left(\frac{1}{r^2}\frac{\partial}{\partial r}(r^2 u_r)\right) = \frac{1}{2G + \lambda}\frac{\partial P}{\partial r} = -\frac{Q_0}{4c\pi}\frac{1}{r^2}. \tag{5.8}$$

The sum of its particular and homogeneous solutions is

$$u_r(r) = \frac{Q_0}{8c\pi} + \frac{D}{r^2} + C r. \tag{5.9}$$

With no contact stress on the boundaries, Eq. (4.7) applies, so that the steady-state displacement distribution is

$$u_r(r) = \frac{Q_0}{16\pi cGr^2}(2Gr^2 + \lambda a^2) = \frac{Q_0}{8\pi c}\left(1 + \frac{\lambda}{2G}\left(\frac{a}{r}\right)^2\right). \tag{5.10}$$

Figure 6 is a plot of $u_r(r)$ vs r/a for parameters given in Table 1. Again, displacement depends upon the material parameters.

6. Step Infusion from a Pressure Source

Now suppose that the pressure in the cavity suddenly jumps from zero to P_0 (i.e., $P(a, t) = P_0 H(t)$, where $H(t)$ is the unit step function). To find the response of the tissue, we integrate the continuity equation, Eq. (2.5), observing that

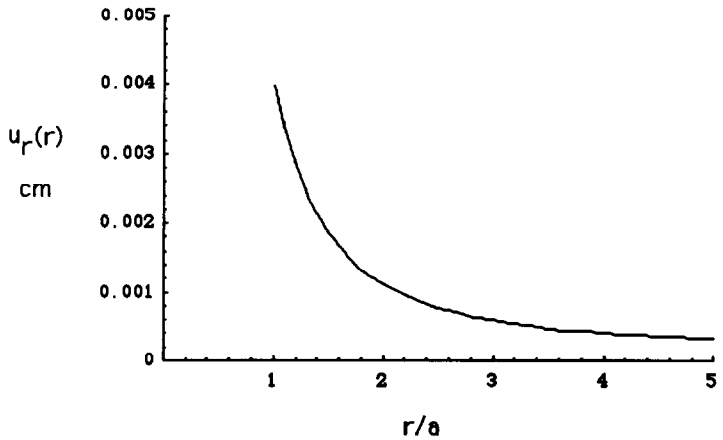

FIG. 6. The steady-state tissue displacement, $u_r(r)$, vs r/a in gray matter for a constant flow-rate infusion.

$$(1 - f)\frac{\partial u_r}{\partial t} + f V_r = \frac{B(t)}{r^2}. \tag{6.1}$$

Eliminating V_r from above using the equation of motion, Eq. (2.3), and Darcy's law, (2.6), we obtain

$$\frac{\partial u_r}{\partial t} = c\frac{\partial}{\partial r}\left(\frac{1}{r^2}\frac{\partial}{\partial r}(r^2 u_r)\right) + \frac{B(t)}{r^2}, \tag{6.2}$$

where $B(t)$ must be determined from initial and boundary conditions.

During the initial instant, $t = 0^+$, the dilatation of the tissue is zero, as in Eq. (3.4); therefore, no fluid enters, leaves, or redistributes itself within the tissue. From Eq. (2.2),

$$r^2 u_r(r,0^+) = A \qquad \text{or} \qquad u_r(r,0^+) = \frac{A}{r^2}. \tag{6.3}$$

Because the dilatation is zero everywhere, Eq. (2.3) implies that the pressure gradient is also zero; therefore, the initial pressure, $P(r,0^+) = P(0^+)$, is uniform within the tissue. The value of $P(0^+)$ is also unknown. Two initial conditions come from the constitutive law, Eq. (1.1):

$$2G\frac{\partial u_r}{\partial r}(a,0^+) + \lambda \cancelto{0}{\theta(a,0^+)} - P(0^+) = -P_0,$$

and

$$2G\frac{\partial u_r}{\partial r}(\infty,0^+) + \lambda \cancelto{0}{\theta(\infty,0^+)} - P(0^+) = 0. \tag{6.4}$$

The conditions are used to calculate $u_r(r,0^+)$ and $P(0^+)$ simultaneously:

$$u_r(r,0^+) = \frac{P_0}{4G}\left(\frac{a^3}{r^2}\right) \qquad \text{and} \qquad P(0^+) = 0. \tag{6.5}$$

The resulting initial internal pressure is zero; the initial displacement field is that of an incompressible, elastic solid subjected to a compressive contact pressure, $-P_0$.

We use the Laplace transform of Eq. (6.2) to obtain a forced, modified spherical Bessel equation,

$$r^2 \frac{\partial^2 u_r}{\partial r^2}(r,s) + 2r \frac{\partial u_r}{\partial r}(r,s) - \left(2 + \frac{s}{c} r^2\right) u_r(r,s) = \alpha(s) \qquad \text{with}$$

$$\alpha(s) = -\left(\frac{P_0 a^3}{4cG} + \frac{B(s)}{c}\right). \tag{6.6}$$

Its analytic solution is

$$u_r(r,s) = \frac{1}{r^2}(-\alpha(s) + C(s)(\sinh r - r\cosh r) + D(s)(\cosh r - r\sinh r)), \tag{6.7}$$

using the substitution

$$r = r\sqrt{\frac{s}{c}}. \tag{6.8}$$

Darcy's law, (2.6), and the equation of continuity, (6.1), relate the pressure gradient and the velocity of the network:

$$\kappa r^2 \frac{\partial P}{\partial r}(r,t) = -B(t) + r^2 \frac{\partial u_r}{\partial t}. \tag{6.9}$$

The Laplace transform of this expression,

$$\kappa r^2 \frac{\partial P}{\partial r}(r,s) = -B(s) + r^2 (s\, u_r(r,s) - u_r(r,0^+)), \tag{6.10}$$

can be integrated with respect to r, simplifying to

$$P(r,s) = -\frac{2G + \lambda}{r}\left(C(s)\sinh\left(r\sqrt{\frac{s}{c}}\right) + D(s)\cosh\left(r\sqrt{\frac{s}{c}}\right)\right) + E(s), \tag{6.11}$$

or

$$P(r,s) = (2G + \lambda)\, e(r,s) + E(s), \tag{6.12}$$

where $E(s)$ is a constant of integration.

Boundary conditions on the interstitial fluid are

$$P(a,s) = \frac{P_0}{s} \qquad \text{and} \qquad P(\infty,s) = 0. \tag{6.13}$$

Boundary conditions on the network are

$$(2G + \lambda)\frac{\partial u_r}{\partial r}(r,s) + \lambda \frac{2u_r(r,s)}{r} = 0 \qquad \text{for } r = a \text{ and } r = \infty, \tag{6.14}$$

i.e., there is no traction on the cavity or at infinity. These four boundary conditions

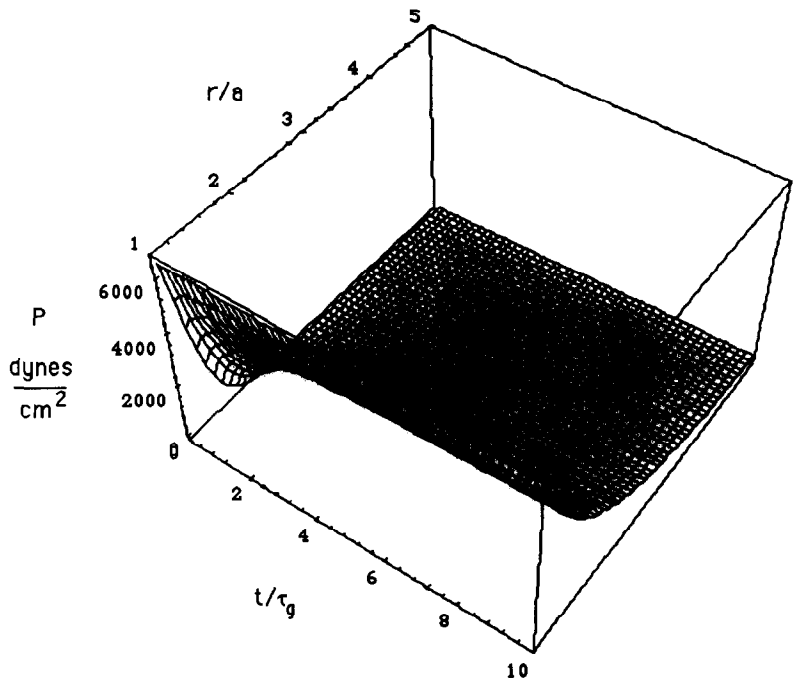

FIG. 7. The tissue pressure distribution, $P(r, t)$, in gray matter vs r/a and dimensionless time, $t/(a^2/c)$.

allow us to solve for the four unknowns $C(s)$, $D(s)$, $E(s)$, and $B(s)$, that are used to calculate the inverse Laplace transforms of the dependent variables $P(r,s)$, $V_r(r,s)$, $e(r,s)$, and $u(r,s)$.

The resulting pressure distribution for $r \geq a$ is

$$P(r,t) = P_0 \frac{a}{r}\left(1 - \operatorname{erf}\left(\frac{r-a}{2\sqrt{ct}}\right)\right). \tag{6.15}$$

It is plotted in Fig. 7 for gray matter.

This closed-form solution suggests a characteristic time constant for diffusion of the dilatation field in an infinite medium,

$$\tau_c = \left(\frac{2a}{\pi}\right)^2 \frac{1}{c}. \tag{6.16}$$

Using Darcy's law, Eq. (2.6), and Eqs. (6.15) and (6.1), we obtain the resulting velocity distribution for $t \geq 0$ and $r \geq a$:

$$V_r(r,t) = \frac{\kappa P_0 a}{r^2}\left(\frac{(1-f)}{f}\left(\operatorname{erfc}\left(\frac{r-a}{\sqrt{4ct}}\right) + \frac{r}{\sqrt{\pi ct}}\exp\left(\frac{-(r-a)^2}{4ct}\right)\right) + \left(1 + \frac{a}{\sqrt{\pi ct}}\right)\right). \tag{6.17}$$

It is plotted in Fig. 8 as a function of time and distance from the core. Initially,

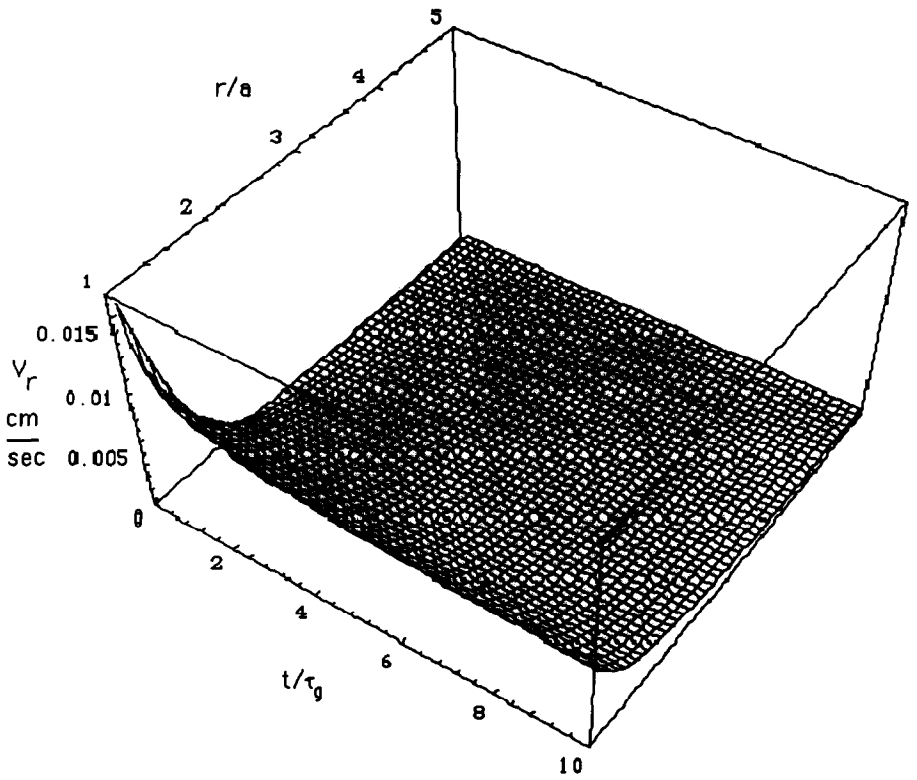

FIG. 8. The interstitial velocity distribution, $V_r(r, t)$, in gray matter vs r/a and $t/(a^2/c)$.

the velocity is large at the fluid/tissue interface, but fluid penetrates only a small distance into the tissue's superficial layers. After a few time constants, the steady-state profile evolves.

We can calculate the dilatation from Eqs. (6.7), (6.8), and (2.2):

$$e(r,s) = \frac{-C(s)\sinh r\sqrt{\frac{s}{c}} - D(s)\cosh r\sqrt{\frac{s}{c}}}{r}. \tag{6.18}$$

This expression satisfies the Laplace-transformed consolidation equation, Eq. (2.7), assuming that the initial dilatation is zero (as in Eq. (6.3)). Its inverse Laplace transform is

$$e(r,t) = \frac{P_0}{2G + \lambda}\frac{a}{r}\left(1 - \operatorname{erf}\left(\frac{r-a}{2\sqrt{ct}}\right)\right). \tag{6.19}$$

The dilatation, calculated with parameters for gray matter, is shown in Fig. 9. The dilatation is positive, indicating a net expansion of tissue volume.

It is easy to obtain the response to an impulse in cavity pressure by taking the time derivatives of the solutions above. For instance, the resulting pressure distribution is given by

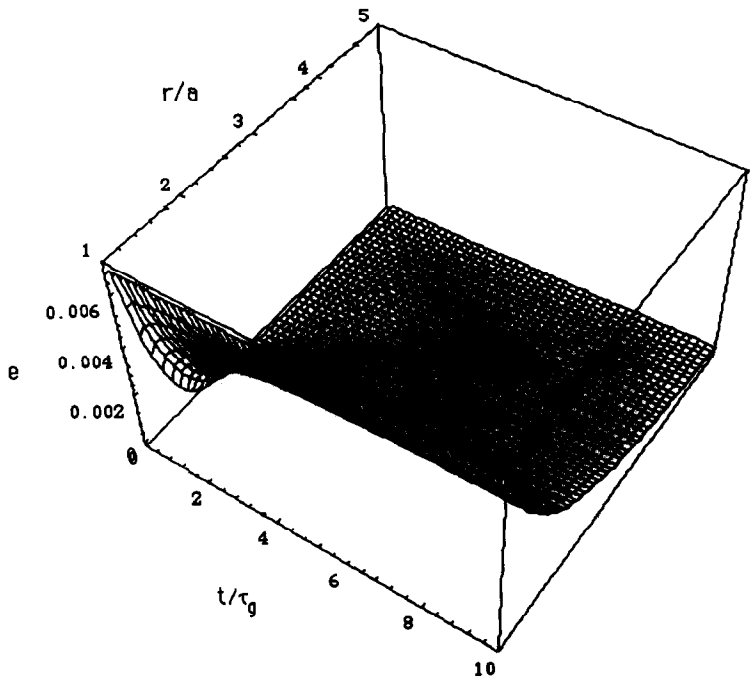

FIG. 9. The tissue dilatation, $e(r, t)$, in gray matter vs r/a and $t/(a^2/c)$.

$$P(r,t) = P_0 \frac{a\,(r-a)\,\kappa}{2\,r\,\sqrt{\pi(ct)^3}} \exp\left(\frac{-(r-a)^2}{4ct}\right). \tag{6.20}$$

7. Step Infusion from a Constant Flow Source

Suppose that a step infusion, $Q(a, t) = Q_0\,H(t)$, is applied to the cavity using a flow source. Then the derivations follow the same steps as before, until we apply boundary conditions. The total stress boundary conditions from Eq. (1.1) are

$$2G\frac{\partial u_r}{\partial r}(r,0^+) + \lambda\cancelto{0}{e(r,0^+)} - P(0^+) = 0 \qquad \text{for } r = a \text{ and } r = \infty. \tag{7.1}$$

These conditions are used to calculate $u_r(r,0^+)$ and $P(0^+)$ simultaneously:

$$u_r(r,0^+) = P(0^+) = 0. \tag{7.2}$$

To find the displacement, we take the Laplace transform of Eq. (6.2), thereby obtaining the same forced, modified spherical Bessel equation as in Eq. (6.6), with

$$\alpha(s) = -\left(\frac{B(s)}{c}\right). \tag{7.3}$$

Its analytic solution is the same as in Eqs. (6.7) and 6.8).

Darcy's law, (2.6), and the equation of continuity, (6.1), are used to relate the pressure gradient and the interstitial velocity:

$$-\kappa\left(\frac{1-f}{f}\right)r^2\frac{\partial P}{\partial r}(r,t) = -B(t) + r^2 V_r(r,t). \tag{7.4}$$

Its Laplace transform is,

$$-\kappa\left(\frac{1-f}{f}\right)r^2\frac{\partial P}{\partial r}(r,s) = -B(s) + r^2 V_r(r,s). \tag{7.5}$$

One boundary condition on the interstitial fluid at $r = a$ comes from imposing a step in flow at the inner boundary:

$$-\kappa\left(\frac{1-f}{f}\right)a^2\frac{\partial P}{\partial r}(a,s) = -B(s) + a^2\left(\frac{Q_0}{sf4\pi a^2}\right). \tag{7.6}$$

The other boundary condition at $r = \infty$ is

$$P(\infty,s) = 0. \tag{7.7}$$

The contact stress on the elastic network is zero, as in Eq. (6.14). Integrating the pressure gradient as before, we obtain Eq. (6.11). Therefore, we can solve Eqs. (7.6), (7.7), and (6.14) for the unknowns $C(s)$, $D(s)$, $E(s)$, and $B(s)$. The resulting transformed expressions are more difficult to invert; however, numerical solutions, e.g., for the dilatation, can be obtained from

$$e(r,t) = \frac{G}{2G+\lambda}\frac{Q_0}{\pi r a^2}\left(\frac{a^2}{4G\kappa} - \frac{1}{\pi}\int_0^\infty \frac{e-t\rho}{\rho}\frac{1}{\left(\frac{4G\kappa}{a^2}-\rho\right)^2 + \left(\frac{4G\kappa}{a\sqrt{c}}\right)^2\rho}\right.$$
$$\left.\left(\left(\frac{4G\kappa}{a^2}-\rho\right)\sin\left(\frac{(-r+a)}{\sqrt{c}}\sqrt{\rho}\right) + \frac{4G\kappa}{a\sqrt{c}}\sqrt{\rho}\cos\left(\frac{(-\mathrm{r}+\mathrm{a})}{\sqrt{c}}\sqrt{\rho}\right)\right)d\rho\right). \tag{7.8}$$

8. Transport and Consolidation in Tissue

Tissue dilatation has already been calculated. Now we relate it to interstitial volume. If a volume of fluid, δV_f, is infused into tissue with an initial volume of V_{0T}, it produces a *tissue* volume change, δV_T. For small deformations, the dilatation of the tissue is related to the initial tissue volume and its volume increment by

$$e = \frac{\delta V_T}{V_{0T}}. \tag{8.1}$$

Since the solid network is assumed to be composed of impermeable, incompressible constituents such as cells and polymer, and since the infusate is incompressible, this increase in fluid volume equals the increase in total tissue volume, i.e.,

$$\delta V_f = \delta V_T. \tag{8.2}$$

Since by definition, $f\,V_{0T} = V_{0f}$,

$$e = \frac{\delta V_T}{V_{0T}} = f\frac{\delta V_f}{V_{0f}}. \tag{8.3}$$

Therefore, the change in interstitial fluid volume per unit undeformed interstitial

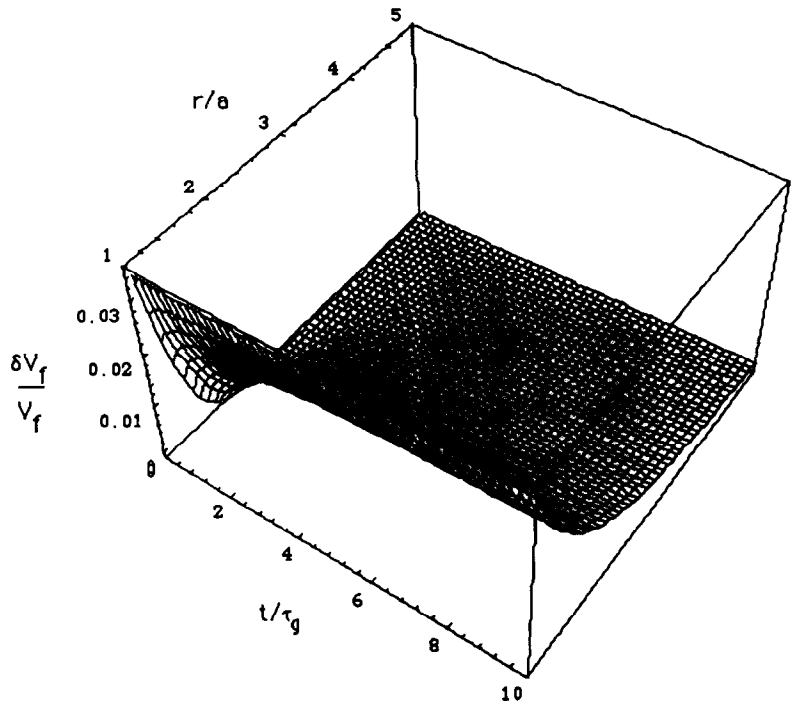

FIG. 10. The fractional change in gray matter interstitial volume, $\delta V_f/V_f\,(r, t)$, vs r/a and $t/(a^2/c)$.

fluid volume (fractional change in interstitial volume) is greater than the change in tissue volume per unit undeformed tissue volume (fractional change in tissue volume) by a factor of the inverse porosity, $1/f$. Typically for white and gray matter, $1/f = 1/0.2 = 5$ [29], so that the fractional interstitial fluid volume increases fivefold for a onefold increase in fractional network volume. For example, an infusion that increases tissue volume by only 5% (which is within the limits of the linear consolidation theory) increases interstitial volume by 25%! A plot of the fractional change in interstitial volume, $\delta V_f/V_{0f}$, from Eq. (8.3), is given for gray matter in Fig. 10.

For small deformations, $\delta V_T \approx V_T - V_{0T}$, so that the relationship between deformed tissue volume, V_T, and initial undeformed tissue volume is

$$V_T \approx V_{0T}\,(1 + e), \tag{8.4}$$

where we have used Eq. (8.3). For small deformations, $\delta V_f \approx V_f - V_{0f}$, the relationship between the fluid volume of the deformed and undeformed tissue, V_f and V_{0f}, is

$$V_f \approx V_{0f}\left(1 + \frac{e}{f}\right). \tag{8.5}$$

Again, the amplification factor $1/f$ appears.

The transport equation for a chemical species in the extracellular space of a porous, nondeformable medium is

$$\frac{\partial C}{\partial t} = D_{\text{eff}} \nabla^2 C - \nabla \cdot (\mathbf{V}\, C) + \phi_s(C, P, t) - \phi_r(C, P, t), \tag{8.6}$$

where C is the local concentration of the solute. The solute flux is ascribed to diffusive and advective transport, consumption, and production. The advective velocity, $\mathbf{V}$, is the same as the local interstitial velocity given in Eq. (1.9). Source and sink terms, $\phi_s(C, P, t)$ and $\phi_r(C, P, t)$, respectively, represent the removal and conversion of the solute and may depend upon pressure, concentration, or time. D_{eff}, the effective diffusivity of the solute in the interstitial space, is assumed to be independent of position.

Equation (8.6) does not apply to a swelling network because its underlying assumption that the elemental volume, $dx\, dy\, dz$, is fixed in space is not satisfied. To include swelling induced by infusion, we require

$$C = C' \frac{V_f}{V_{0f}} = C' \left(1 + \frac{e}{f}\right), \tag{8.7}$$

where C' is the interstitial concentration in the deformed network. Then the equation becomes

$$\frac{\partial C' \left(1 + \frac{e}{f}\right)}{\partial t} = -\nabla \cdot \left(\mathbf{V}\, C' \left(1 + \frac{e}{f}\right)\right) + D_{\text{eff}} \nabla^2 C' \left(1 + \frac{e}{f}\right) + \phi_s\left(C' \left(1 + \frac{e}{f}\right), P, t\right) - \phi_r\left(C' \left(1 + \frac{e}{f}\right), P, t\right). \tag{8.8}$$

This transport equation explicitly includes tissue dilatation. Changes in interstitial volume during infusion affect transport of solutes within the interstitium by: (i) altering local bulk flow (advection), (ii) diluting the solute, (iii) altering reaction kinetics (such as binding), and (iv) reducing concentration gradients (diffusion). Other potentially important effects not included here are changes in solute diffusivity or material constants of the tissue (such as the permeability, shear modulus, or Lamé constant) caused by swelling. It should also be noted that when $e = 0$, the transport equation reduces to Eq. (8.6).

DISCUSSION

The time of mechanical relaxation of the pressure, displacement, velocity, and dilatation fields arises naturally when tissue deformation is seen as a diffusive process. By analogy with other consolidation problems [9,11,12], the characteristic consolidation time constant for a finite spherical shell of brain tissue is $\tau_c \sim (R_o - a)^2/c$, where R_o is the shell's outer radius. Time constants for diffusion, advection, and consolidation are given in Table 2, using the proposed parameters for gray and white matter given in Table 1 and assuming $R_o = 2$ cm. Peclet numbers near the cavity and at the periphery are calculated. Large Peclet numbers for gray and white matter near the cavity show that bulk solute transport dominates diffusive transport there, in accord with the estimates of Morrison *et al.* [1]. Interestingly, convective transport still dominates at the periphery, although diffusion is relatively more important there. Another group, *AS*, which is the di-

TABLE 2
TIME CONSTANTS FOR DIFFERENT PHYSICAL AND CHEMICAL PROCESSES

Process	Time constant	Gray matter (sec)	White matter (sec)
Consolidation	$\tau_c = \left(\frac{2}{\pi}\right)^2 \frac{(R_o - a)^2}{c}$	335	500
Diffusion	$\tau_d = \left(\frac{2}{\pi}\right)^2 \frac{(R_o - a)^2}{D}$	2×10^7	2×10^7
Advection (periphery)	$\tau_{ap} = \frac{f(R_o - a)^3}{a\kappa P_o}$	1.5×10^6	1×10^6
Advection (cavity)	$\tau_{ac} = \frac{fa^2}{\kappa P_o}$	5	3

mensionless ratio of swelling and advective time constants, predicts whether the initial or the steady-state conditions dictate the velocity distribution used in the transport equation.

These analytic solutions for steady and step infusions also can be used to assess the credibility of published estimates of material properties of gray and white matter. For instance, Nagashima cites $E_g = 30$ dynes/cm^2 and $\nu_g = 0.4999$ in gray matter, and $E_w = 3$ dynes/cm^2 and $\nu_w = 0.4999$ for white matter [5]. These material constants correspond to $G_g = 10$ dynes/cm^2 and $\lambda_g = 50{,}000$ dynes/cm^2 for gray matter, and $G_w = 1.0$ dynes/cm^2 and $\lambda_w = 5000$ dynes/cm^2 for white matter. When these parameters are used to describe the response of brain tissue to a step-infusion of 6664 dynes/cm^2 (approximately 5 mm Hg), one predicts initial cavity displacements, $P_0a/(4G)$, that are many times the initial radius. It is likely that Nagashima's G_g and G_w are too small. They should be on the order of 7000 dynes/cm^2. Perhaps the cited G and λ are not the "final" equilibrium

TABLE 3
USEFUL DIMENSIONLESS GROUPS

	Dimensionless	Gray Matter	White Matter
Peclet Number (per.)	$\mathrm{Pe} = \frac{a\kappa P_o}{(R_o - a)Df}$	25	38
Peclet Number (cav.)	$\mathrm{Pe} = \frac{\kappa P_o (R_o - a)^2}{Da^2 f}$	7×10^6	1×10^7
Advect./Swell. (per.)	$\mathrm{AS} = \frac{a\kappa P_o}{(R_o - a)cf}$	5×10^{-4}	1×10^{-3}
Advect./Swell. (cav.)	$\mathrm{AS} = \frac{\kappa P_o (R_o - a)^2}{ca^2 f}$	152	343

moduli [9,11,12,14] required in the Biot model. Hydraulic "conductivity" is given as 10^{-11} cm^3/dynes-sec in gray matter and 10^{-9} cm^3/dynes-sec in white matter [5]. It is not clear how to convert them to the Darcy permeability, κ, that is, in units of cm^4/dynes-sec. Unfortunately, it is difficult to resolve these disagreements because there are few published measurements of material constants of brain tissue.

To address this problem, it is possible to estimate material constants of poroelastic tissue with this model using time-varying infusion protocols. If χ^2 is the weighted sum of squares of the deviations between $N \times M$ experimental and model-generated pressure data points, i.e.,

$$\chi^2 = \sum_{i=1}^{N} \sum_{j=1}^{M} \frac{(P_{\text{model}}(r_i, t_j) - P_{\text{experiment}}(r_i, t_j))^2}{\sigma_{ij}^2}, \tag{9.1}$$

where σ_{ij}^2 are the error variances, then we can estimate optimal material parameters, κ_{opt} λ_{opt}, and G_{opt} by minimizing χ^2 with respect to κ, λ, and G. This method was used recently to estimate material constants of hydrogels [30].

Taylor *et al.* [2,3] used tissue compliance to relate changes in interstitial pressure to changes in volume rather than the equations of motion of the tissue, Eq. (1.5), and boundary conditions for the pressure and contact stress, e.g., Eqs. (3.1)–(4)—Newton's second and third laws. The utility of the Taylor model appears to be limited to cases in which there is no relative flow of interstitial fluid and the elastic network, and in which the pressure and contact stress are zero at all boundaries. Certainly, changes in CSF pressure or contact forces exerted by the skull cannot be described. Modeling *in vitro* experiments in which the tissue sample is held in a fixture is also problematic.

However, an interesting connection can be made between the Taylor and the Biot models. Specific tissue compliance, C_t [2,3], can be determined from the Biot model using analytic expressions relating pressure and dilatation, e.g., Eq. (6.12):

$$C_t = \frac{\partial e}{\partial P} = \frac{1}{2G + \lambda}. \tag{9.2}$$

Here we see that C_t is the reciprocal effective modulus of the elastic network (e.g., as in Eq. (1.8)). Generally, specific tissue compliance depends on initial and boundary conditions [14], tissue geometry and composition, and the form of the constitutive law, so that C_t is not a material property. A more general relationship between e and P for the linear poroelastic model is given in Eq. (1.8). Inclusion of vascular compliance would also change the form of Eq. (9.2).

The present model does not describe fluid leakage around a needle that is used to deliver fluid to the cavity. When the infusion pressure is high enough, a low-impedance pathway may open along the needle shaft, shunting fluid from the cavity. If the cavity were formed by a needle tip, then it may be tear-shaped, not spherical. To assess the validity of the assumption of spherical symmetry and small deformations, a three-dimensional, finite element analysis and careful experiments need to be performed. This is beyond the scope of the present paper. Nonetheless, the analytical solutions presented above should predict the correct

qualitative behavior for the assumed material properties and can be used to validate predictions obtained using numerical methods.

CONCLUDING REMARKS

Time-varying flow and pressure sources can be considered in the future. Enhanced mass transfer may occur by superposing AC and DC pressure or flow wave forms. It will also be interesting to predict the transport of a solute following the cessation of fluid infusion and to consider the case in which tissue is attached (glued) to the needle. In this instance, the local tissue displacement at the cavity/tissue interface is zero, although the fluid velocity there is not. This case is not considered here because it is less clinically relevant and would make this paper unreasonably long.

Incorporating empirically derived relationships between hydraulic permeability and pore fraction, $\kappa(f)$, should extend the applicability of this model. Another promising extension would be to incorporate the anisotropy of white matter. Finally, swelling induced by infusion may affect the distribution of other infused agents such as proteins, nucleic acids, viruses, and cells.

ACKNOWLEDGMENTS

The National Cancer Institute (NCI) allocated computing time and staff support at the Advanced Scientific Computing Laboratory of the Frederick Cancer Research Facility that permitted numerical calculations to be performed. Thanks go to Bob Dedrick and Paul Morrison, BEIP, whose novel proposal that chemotherapeutic agents can be infused into brain tissue motivated this work. Paul also read portions of this paper carefully and provided technical assistance and encouragement. Jeffrey Sachs, NIST, read this paper carefully and made numerous insightful suggestions. Richard Chadwick of BEIP also made helpful suggestions. Barry Bowman carefully edited this manuscript.

REFERENCES

1. Morrison, P., Dedrick, B., and Laske, D. (1991). Personal communication.
2. Taylor, D. G., Bert, J. L., and Bowen, B. D. (1990a). A mathematical model of interstitial transport. I. Theory. *Microvasc. Res.* **39,** 253–278.
3. Taylor, D. G., Bert, J., and Bowen, B. D. (1990b). A mathematical model of interstitial transport. II. Microvascular exchange in mesentery. *Microvasc. Res.* **39,** 279–306.
4. Nicholson, C. (1985). Diffusion from an injected volume of a substance in brain tissue with arbitrary volume fraction and tortuosity. *Brain Res.* **333,** 325–329.
5. Nagashima, T., Tamaki, N., Matsumoto, S., Horwitz, B., and Seguchi, Y. (1987). Biomechanics of hydrocephalus: A new theoretical model. *Neurosurgery.* **21,** 898–904.
6. Nagashima, T., Horwitz, B., and Rapoport, S. I. (1990a). A mathematical model for vasogenic brain edema. *Adv. Neurol.* **52,** 317–326.
7. Nagashima, T., Shirakuni, T., and Rapoport, S. I. (1990b). A two-dimensional finite element analysis of vasogenic brain edema. *Neurol. Med. Chir. (Tokyo)* **30,** 1–9.
8. Nagashima, T., Tada, Y., Hamano, S., Skakakura, M., Masaoka, K., Tamaki, N., and Matsumoto, S. (1990c). The finite element analysis of brain oedema associated with intracranial meningiomas. *Acta Neurochir. Suppl. (Wien).*
9. Biot, M. A. (1941). General theory of three-dimensional consolidation. *J. Appl. Phys.* **12,** 155–164.
10. Biot, M. A. (1955). Theory of elasticity and consolidation for a porous anisotropic solid. *J. Appl. Phys.* **26,** 182–185.

11. BIOT, M. A., AND CLINGAN, F. M. (1941). Consolidation settlement of a soil with an impervious top surface. *J. Appl. Phys.* **12,** 578–581.
12. BIOT, M. A. (1941). Consolidation settlement under a rectangular load distribution. *J. Appl. Phys.* **12,** 426–430.
13. BIOT, M. A. (1956). General solutions of the equations of elasticity and consolidation for a porous material. *J. Appl. Phys.* **78,** 91–96.
14. BIOT, M. A., AND WILLIS, G. (1957). The elastic coefficients of the theory of consolidation. *J. Appl. Mech.* **24,** 594–601.
15. KENYON, D. E. (1979). A mathematical model of water flux through aortic tissue. *Bull. Math. Biol.* **41,** 79–90.
16. JAYARAMAN, G. (1983). Water transport in the arterial wall—A theoretical study. *J. Biomech.* **16,** 833–840.
17. JAIN, R., AND JAYARAMAN, G. (1987). A theoretical model for water flux through the arterial wall. *J. Biomech. Eng.* **109,** 311–317.
18. SALZSTEIN, R. A., POLLACK, S. R., MAK, A. F. T., AND PETROV, N. (1987). Electromechanical potentials in cortical bone. I. A continuum approach. *J. Biomech.* **20,** 261–270.
19. MOW, V. C., AND LAI, W. M. (1979). Mechanics of animal joints. *Annu. Rev. Fluid Mech.* **11,** 247–288.
20. JOHNSON, D. L. (1982). Elastodynamics of gels. *J. Chem. Phys.* **77,** 1531–1539.
21. GRIMSHAW, P. E., GRODZINSKY, A. J., YARMUSH, M. L., AND YARMUSH, D. M. (1989). Dynamic membranes for protein transport: Chemical and electrical control. *Chem. Eng. Sci.* **44,** 827–840.
22. RICE, J. R., AND CLEARY, M. P. (1976). Some basic stress diffusion solutions for fluid-saturated elastic porous media with compressible constitutents. *Rev. Geophys. Space Phys.* **14,** 227–241.
23. TERZAGHI, K. (1923). Die Berechung der Durchassigkeitsziffer des Tones an dem Verlauf der hydrodynamischen Spannungserscheinungen. *Sitzungsber. Akad. Wiss. Wien Math. Naturwiss. Kl. Abt.* **2A,** 105.
24. TERZAGHI, K. (1925). "Erdbaumechanik auf Bodenphysikalischen Grundlagen." Deuticke, Vienna.
25. EISENBERG, S. R., AND GRODZINSKY, A. J. (1985). Swelling of articular cartilage and other connective tissue: electromechanochemical forces. *J. Orthop. Res.* **3,** 148–159.
26. RAPOPORT, S. I., OHNO, K., AND PETTIGREW, K. D. (1979). Drug entry into the brain. *Brain Res.* **172,** 354–359.
27. KENYON, D. E. (1976). Transient filtration in a porous elastic cylinder. *Trans. ASME J. Appl. Mech.* **98,** 594–598.
28. TANAKA, T., AND FILLMORE, D. J. (1978). Kinetics of swelling of gels. *J. Chem. Phys.* **70,** 1214–1218.
29. NICHOLSON, C., AND PHILLIPS, J. M. (1981). Ion diffusion modified by tortuosity and volume fraction in the extracellular microenvironment of the rat cerebellum. *J. Physiol.* **321,** 225–257.
30. CHIARELLI, P., BASSER, P. J., DEROSSI, D., AND GOLDSTEIN, S. R. The dynamics of a gel strip. *Biorheology,* in press.